HHS Public Access

Author manuscript

Neuroscience. Author manuscript; available in PMC 2016 August 20.

Published in final edited form as:

Neuroscience. 2015 August 20; 301: 71–78. doi:10.1016/j.neuroscience.2015.05.078.

NEURONAL HYPOXIA DISRUPTS MITOCHONDRIAL FUSION

T. H. SANDERSON[a,b], **S. RAGHUNAYAKULA**[a], and **R. KUMAR**[a,b,c,*]

[a]Department of Emergency Medicine, Wayne State University School of Medicine, 540 E. Canfield, Detroit, MI, USA

[b]Cardiovascular Research Institute, Wayne State University School of Medicine, 421E. Canfield, Detroit, MI, USA

[c]Department of Physiology, Wayne State University School of Medicine, 540 E. Canfield, Detroit, MI, USA

Abstract

Brain ischemia/reperfusion injury results in death of vulnerable neurons and extensive brain damage. It is well known that mitochondrial release of cytochrome *c* (cyto *c*) is a hallmark of neuronal death, however the molecular events underlying this release are largely unknown. We tested the hypothesis that cyto *c* release is regulated by breakdown of the cristae architecture maintenance protein, optic atrophy 1 (OPA1), located in the inner mitochondrial membrane. We simulated ischemia/reperfusion in isolated primary rat neurons and interrogated OPA1 release from the mitochondria, OPA1 oligomeric breakdown, and concomitant dysfunction of mitochondrial dynamic state. We found that ischemia/reperfusion induces cyto *c* release and cell death that corresponds to multiple changes in OPA1, including: (i) translocation of the mitochondrial fusion protein OPA1 from the mitochondria to the cytosol, (ii) increase in the short isoform of OPA1, suggestive of proteolytic processing, (iii) breakdown of OPA1 oligomers in the mitochondria, and (iv) increased mitochondrial fission. Thus, we present novel evidence of a connection between release of cyto *c* from mitochondria and disruption of the mitochondrial fusion.

Keywords

cytochrome *c*; ischemia; reperfusion; mitochondrial dynamics; oxidative stress; brain

INTRODUCTION

Brain ischemia and reperfusion injury continue to be a leading cause of loss of cerebral function following cardiac arrest or stroke, often resulting in mortality. In neurons, post-ischemic cell signaling often culminates on the mitochondria resulting in the detrimental release of cytochrome *c* (cyto *c*) from mitochondria (Perez-Pinzon et al., 1999; Sugawara et al., 1999; Prakasa Babu et al., 2000; Borutaite et al., 2003). Many investigators have

*Correspondence to: R. Kumar, Wayne State University School of Medicine, Elliman Building, Room 1224, 421 E. Canfield, Detroit, MI 48201. USA. Tel: +1-313-577-5738. rkuma@med.wayne.edu (R. Kumar). .

proposed and tested a number of hypotheses centered on mitochondrial rupture, pro-apoptotic pore formation, and/or mitochondrial permeability transition as the basis of cyto *c* release into the cytosol following brain ischemia (Borutaite et al., 2003; Hirakawa et al., 2003; Zhao et al., 2005; Endo et al., 2006). Although there has been a great deal of research on this topic, there is little consensus in the field regarding the specific mechanism of cyto *c* release from mitochondria following cerebral ischemia.

The emergent field of mitochondrial dynamics has revealed that mitochondria are dynamic and continuously exist in a balance of fission and fusion phenotypes in response to stimuli in the cellular environment (Chen and Chan, 2004; Chan et al., 2006). While mitochondria typically exist as both thread-like and granular structures, genetic manipulation of eukaryotic cells that push mitochondrial phenotypes into either extreme allowed the identification of key proteins that regulate mitochondrial dynamics. Mitochondrial fission and fusion are highly regulated processes that are controlled by a wide array of signaling mechanism including post-translational modifications, cellular localization changes, and proteolytic cleavage of the key regulatory proteins. Interestingly, recent studies have implicated severe alterations in mitochondrial dynamic phenotype as a key regulator of the apoptotic program (cyto *c* release) (Nguyen et al., 2011). Considering alterations in mitochondrial dynamics occur in response to physiological changes in cells and severe cellular stress can unbalance mitochondrial dynamics to favor cell death, we investigated the concept that mitochondrial dynamics could play a key role in neuronal apoptosis following ischemia/reperfusion.

We, like others, have observed cyto *c* release following global brain ischemia (Perez-Pinzon et al., 1999; Namura et al., 2001; Sanderson et al., 2008, 2013). To clearly observe if alterations in mitochondrial morphology and dynamics play a role in cyto *c* release, we chose to interrogate a key regulator of mitochondrial fusion, optic atrophy 1 (OPA1), and mitochondrial dynamics in primary hippocampal and cortical rat neurons subjected to oxygen–glucose deprivation. This model allows for clear visualization in alterations of mitochondria of neurons in a relatively homogenous environment. Here we report that oxygen–glucose deprivation in primary neuronal culture results in release of cyto *c* from mitochondria, with concomitant release of OPA1 into the cytosol, breakdown of OPA1 complexes, excessive mitochondrial fragmentation, and neuronal death.

EXPERIMENTAL PROCEDURES

Preparation of cortical neurons

All experiments conformed to Wayne State University's animal care program as well as International Guidelines on the ethical use of animals and that all efforts were made to minimize the number of animals used and their suffering. Primary cultures of cortical and hippocampal neurons were isolated from embryonic day 18 Sprague–Dawley rats using a modification of Hilgenberg and Smith (2007). In brief, cerebral cortices and hippocampi were isolated in ice-cold dissection buffer, and incubated in papain. The tissue was then gently triturated in ice-cold Hibernate E medium (Invitrogen). After the tissue settled, the supernatant was aspirated, and the cells were resuspended in Neurobasal Media with B27 supplement (Invitrogen). Cells were plated on poly-D-lysine-coated plates and kept at 37 °C

in a 5% CO_2 incubator. After 4–6 days *in vitro*, half the media was replaced and cultures were fed every 3–4 days. All experiments were performed with a mixture of cortical and hippocampal neurons (subsequently referred to as primary neurons) and were used at 10–15 days *in vitro*. These cultures were 91–95% neuronal, as estimated by immunocytochemical staining according to the manufacturer's protocols with anti-MAP2 antibody (1:10,000; #ab5392; Abcam Cambridge, MA, USA).

Oxygen–glucose deprivation model

To model ischemia-like conditions *in vitro*, cells were exposed to transient oxygen and glucose deprivation (OGD) (modification of (Scorziello et al., 2001)). In brief, the culture medium was replaced two times with serum- and glucose-free medium bubbled with 95% nitrogen and 5% CO_2, resulting in a final glucose concentration of <1 mM. The glucose-deprived cultures were then placed in a Billups-Rothenberg (Del Mar, CA, USA) modular incubator chamber, which was flushed for 10 min with 95% nitrogen and 5% CO_2 and then sealed. The chamber was placed in a water-jacketed incubator at 37 °C for 60 min and then returned to 95% air, 5% CO_2 and glucose-containing medium for the period of time indicated in each experiment. Control glucose-containing cultures were incubated for the same periods of time at 37 °C in humidified 95% air and 5% CO_2.

Cellular fractionation

Mitochondria were isolated from cells according to previously described methods with modifications (Almeida and Medina, 1997, 1998; Kristian et al., 2006). In brief, primary neurons were rinsed with phosphate-buffered saline (PBS) and collected in mitochondria isolation buffer (MIB) containing 210 mM mannitol, 70 mM sucrose, 10 mM HEPES, pH 7.5, 1 mM EGTA, 1 mM EDTA, 100 mM KCl, protease and phosphatase inhibitors. Neurons were homogenized using a Teflon-homogenizer to break open the cells, and centrifuged at 1000*g* for 10 min. The supernatant was transferred to be centrifuged at 10,000*g* for 15 min to collect the mitochondria. The remaining supernatant was collected as the cytosolic fractionand stored at −80 °C. The mitochondrial pellet was resuspended in MIB containing 1% triton X-100 and stored at −80 °C.

Western blots

Protein concentration was determined using the Coomassie protein assay (#1856209; Thermo scientific, Rockford, IL, USA) according to the manufacturer's instructions. Equal amounts of protein were denatured in sodium dodecyl sulfate (SDS) sample buffer (Boston BioProducts, Ashland, MA, USA; #BP-111R) and resolved by SDS–polyacrylamide gel electrophoresis (8–12% polyacrylamide), transferred to nitrocellulose membranes and analyzed for OPA1 (1:1,000; #612607; BD Biosciences, San Jose, CA, USA) and cyto *c* (1:1000; 556433; BD Biosciences, San Jose, CA, USA), glyceraldehyde 3-phosphate dehydrogenase (GADPH) (1:2000; #G8795; Sigma, St. Louis, MO, USA), and adenosine triphosphate (ATP) synthase (1:1000; #ab14730; Abcam, Cambridge, MA, USA) by Western blotting using the enhanced chemiluminescence technique (#32132; Pierce, Rockford, IL, USA). In the figures, each lane represents one experiment. The data were represented as mean ± SD from three experiments. Relative band densities were determined

by densitometry and groups were compared using a one-way ANOVA followed by Tukey's HSD test for post hoc analysis to statistically evaluate differences between groups.

Blue Native-Polyacrylamide Gel Electrophoresis (BN-PAGE)

Blue native electrophoresis was utilized to isolate membrane protein complexes and analysis of molecular masses and oligomeric states of protein complexes, as described (Hornig-Do et al., 2009). Linear 5–13% (w/v) polyacrylamide-gradient gels were formed with a 4% overlay. Proteins were extracted from mitochondrial samples using Lauryl maltoside (2:1 wt:wt sample protein). Samples were supplemented with a fivefold concentrated loading dye (5% Serva Blue G, 750 mM 6-amino-n-caproic acid and 100 mM bis-Tris, pH 7.0). The electrophoresis was started at 100 V for and increased to 240 V once samples entered into the overlay gel at room temperature. Native gels were transferred to nitrocellulose membranes and de-stained of Coomassie brilliant blue with methanol prior to immunoblotting. Immunoblotting was performed as described in Western blot section above using anti-OPA1 antibodies.

Immunofluorescence

Primary neurons were transfected with a mitochondrial marker, the pAcGFP1-Mito Vector (#632432, Clonetech Laboratories, Inc., Mountain View, CA, USA) referred to as mito green fluorescent protein (mitoGFP), using Lipofectamine 2000 (#11668-027, Invitrogen, Grand Island, NY, USA) according to the manufacturer's instructions. Primary neurons were then exposed to 1 h OGD followed by 1 or 6 h of reoxygenation. At the appropriate reoxygenation time, primary neurons were rinsed with PBS and fixed with 4% paraformaldehyde for 15 min at 37 °C.

Coverslips were incubated in permeabilization/blocker solution (5% horse serum [#26050; Gibco] in 0.3% Triton-X100/PBS) for 1 h, and coverslips were incubated in primary antibody against cyto *c* (1:100; #ab110325; Abcam, Cambridge, MA, USA), followed by Alexa Fluor 546 (1:200; #A11003 Invitrogen, Grand Island, NY, USA) secondary antibody. Coverslips were mounted using Vectorshield mounting media (#H-1200; Vector Laboratories, Burlingame, CA, USA) containing 4′,6-diami dino-2-phenylindole (DAPI) that counterstained the nuclei on glass slides. Coverslips were examined under a fluorescence AxioObserver inverted fluorescence microscope (Carl Zeiss Microscopy, Jena, Germany) equipped with objective lens 63×/1.40 oil (λ_{ex}:488 nm; λ_{em}: 515–530 nm). Images of mitochondrial morphology were captured using an AxioCam MRm camera (Carl Zeiss Microscopy, Jena, Germany).

Only primary neurons transfected with the mitoGFP were imaged to identify localization of cyto *c* in these cells. Colocalization of cyto *c* and mitoGFP was analyzed using the Pearson's coefficient analysis in Image J software (Bolte and Cordelieres, 2006).

Mitochondrial morphology

For detection of mitochondrial morphology changes in control and experimental groups, primary neurons were plated on coverslips, exposed to control or 1-h OGD followed by 6-h reoxygenation. The coverslips were then incubated with 100 nM Mitotracker RedFM

(#M22425, Invitrogen, Grand Island, NY, USA) as per the manufacturer's instructions. Live images of mitochondrial morphology were captured using an AxioCam MRm camera mounted to a fluorescence AxioObserver inverted fluorescence microscope (Carl Zeiss Microscopy, Jena, Germany) equipped with objective lens 63×/1.40 oil (λ_{ex}:488 nm; λ_{em}: 515–530 nm).

Counting of two different types of mitochondrial morphology states was performed as previously describe (Sanderson et al., 2015). In brief, quantification in at least three independent experiments with 50 cells per condition in $n = 4$ coverslips by three independent investigators blinded toward the experimental groups were analyzed. The two categories of cells were characterized by their contrasting mitochondrial morphology states and were defined as follows: category 1 were cells displaying mitochondria in an elongated tubular network with some smaller mitochondria; these mitochondria are equally distributed throughout the cytosol. Category 2 were cells contain smaller round mitochondria located close to the nucleus. For statistical analysis, the experiments were repeated at least three times.

Statistics

All data and experiments described in the present study were repeated multiple times, and only one set of representative data is shown. Standard deviation (SD) was used to reflect the variation of the replicate determinations. Data were fit by linear regression and groups are compared using a one-way ANOVA of regression lines followed by a Tukey's HSD test for post hoc analysis to statistically evaluate differences between groups (GraphPad Prism, La Jolla, CA, USA).

RESULTS

We began our study by establishing that 1 h of OGD followed by 24 h of reoxygenation in glucose rich media lead to death of primary neurons in our hands. To quantify the potency of this insult we measured lactate dehydrogenase (LDH) release in experimental versus control cells and normalized these measurements to total LDH release by triton X-100. In control samples, there was 15% LDH release compared to the 96% LDH release in the experimental groups (Fig. 1A; $p < 0.05$). Following 24 h of reoxygenation in experimental groups, cells underwent a gross morphological change as seen by brightfield microscopy and trypan blue staining (Fig. 1B) indicating that indeed 1 h of OGD had a substantial impact on the overall survival of primary neurons when compared to controls.

OGD induces cyto *c* and OPA1 release from mitochondria into the cytosol

The small heme protein, cyto *c*, resides predominantly in the cristae folds of mitochondrial intermembranous space. It is an integral part of the electron transport chain (ETC), and when released from the mitochondria, activates a cascade of events leading to demise of the cell. Therefore we investigated the effect of OGD on mitochondrial cyto *c* release in primary neurons. Following OGD and defined durations of reoxygenation, primary neurons were separated into mitochondrial and cytosolic fractions and proteins were resolved by SDS–PAGE. Western blot analysis of control, 1-h OGD followed by 1 and 6 h of reoxygenation

in glucose rich media samples were conducted probing for cyto *c* (Fig. 2A). In control neurons, cyto *c* was predominantly in the mitochondrial fraction and little was present in the cytoplasmic fraction. Following 1-h OGD and 1-h reoxygenation, cyto *c* still remained in the mitochondrial fraction. However, by 6 h of reoxygenation following 1-h OGD, there was a significant increase in cyto *c* in the cytoplasmic fraction (Fig. 2B; $p < 0.05$). This was accompanied by a significant decrease in cyto *c* in the corresponding mitochondrial fraction.

The majority of cyto *c* resides in the cristae structures of the intermembranous space between the inner and outer mitochondrial membranes. Cristae are invaginations of the inner mitochondrial membrane (IMM) that aid in increasing the surface area of the fundamental site of oxidative phosphorylation. Cristae junctions are formed when two segment of IMM abut one another and are held intact by oligomers of the "gate-keeping" protein, OPA1. OPA1 long and short isoforms oligomerize to form cristae junctions. To investigate if the release of cyto *c* from the mitochondria was related to OPA1, we probed mitochondrial and cytosolic fractions of primary neurons subjected to 1 h of OGD followed by 1- or 6-h reoxygenation. The oligomers of OPA1 that exist in long and short isoforms are typically associated with the IMM. Following OGD we observed OPA1 in the cytoplasm at 1-h reperfusion and a large increase of OPA1 in the cytoplasm at 6-h reperfusion (band 4, Fig. 2C, D; $p < 0.05$). In mitochondrial fractions, at 6 h of reperfusion there was decrease in higher molecular weight isoforms of OPA1 that are seen in controls (bands 1–3, Fig. 2C, D; $p < 0.05$) suggesting that long isoforms of OPA1 were being cleaved and visibly out of the mitochondria into the cytoplasm.

We then went on to measure if there was any overall change in OPA1 expression in whole cell homogenates. We reduced resolution of bands in our Western blot analysis of OPA1 in comparison to our Western blot that can identify individual bands (Fig. 2C) in order to analyze the cluster of OPA1 bands together. There was no significant difference in overall expression of OPA1 following OGD and 1- and 6-h reperfusion in comparison to controls (Fig. 2E, F; $p < 0.05$).

Simulated ischemia in primary neurons results in breakdown of OPA1 oligomers

Constitutive processing of OPA1 results in long and short forms that oligomerize to form a lattice that maintains the cristae junction. Release of OPA1 from mitochondria would suggest interruption in the OPA1 lattice. We next used BN-PAGE to identify the oligomeric state of OPA1 following 1-h of OGD and 6-h reoxgenation in glucose rich media. Western blot analysis of the intact mitochondrial OPA1 complexes demonstrated significant breakdown in the OPA1 complex following simulated ischemia/reperfusion (Fig. 3; $p < 0.05$). Reduction in the OPA1 complexes at 6 h post-OGD, coincides with release of OPA1 from the mitochondria.

Simulated ischemia in primary neurons results in fragmented mitochondria

The dynamin-like GTPase OPA1 functions to maintain cristae junctions, but importantly is a key protein in mitochondrial fusion events. Mitochondrial dynamics, fusion and fission events, are highly regulated occurrences in response to fluctuating physiological cues. Interruption in mitochondrial fusion would result in a predominantly fission phenotype, and

conversely, breakdown in fission would result in a network of fused mitochondria. To visualize if breakdown of OPA1 oligomers, and release of OPA1 would have a morphological effect on mitochondria, we analyzed gross mitochondrial morphology utilizing Mitotracker Red in control primary neurons and following 1-h OGD followed by 6-h reoxygenation in glucose rich media. Utilizing confocal microscopy, we imaged neurons to evaluate the overall morphology of mitochondria and quantify the number of cells with either interconnected tubular mitochondria with some granular mitochondria (category 1) or cells with a dominant small, fragmented mitochondrial morphology (category 2) (Fig. 4). In control cells, mitochondria were filamentous and found throughout the entire neuronal cell body and processes. In the OGD-exposed experimental group, mitochondria were fragmented and granular in appearance, and were located primarily in the soma (Fig. 4; $p < 0.05$). This indicates that OGD induces a dominant fragmented/fission phenotype.

Simulated ischemia in primary neurons results in concomitant cyto *c* release and fragmented mitochondria

Finally, we assessed cyto *c* localization in relationship to mitochondria following OGD and reoxygenation. MitoGFP transfected primary neurons in control and following 1-h OGD with 1- or 6-h reoxygenation in glucose rich media were probed for cyto *c*. In control cells, mitochondria were tubular and cyto *c* immunofluorescence completely superimposed on the mitoGFP signal with a Pearson's correlation coefficient of $r = 0.97$ (Fig. 5, Row 1), indicating cyto *c* was only present in the mitochondria. At 1-h OGD and 1-h reoxygenation, mitochondria appeared smaller, however, the cyto *c* signal completely overlapped with the mitoGFP signal, Pearson's correlation coefficient $r = 0.99$ (Fig. 5, Row 2). At 6-h reoxygenation, mitochondria were completely fragmented, analogous to that detected with Mitotracker (Fig. 4). Furthermore, cyto *c* signal could be seen throughout the cytoplasm which is in agreement with our Western blot data (Fig. 2A). The merge of the mitoGFP signal and cyto *c* (Fig. 5, Row 3), demonstrates release of cyto *c* from the mitochondria, Pearson's correlation coefficient $r = 0.45$.

DISCUSSION

The structural architecture of the mitochondria is unique in that it is enclosed by an outer mitochondrial membrane but is segregated into two distinct compartments by an IMM. The IMM contains a number of folds, cristae, which increase the internal surface area of the IMM (Perkins et al., 1997). It is this large surface area of the cristae that accommodate the protein complexes that form the ETC (Acin-Perez et al., 2008). Most of the components of the ETC are transmembrane proteins, confined to the IMM to efficiently shuttle protons from the mitochondrial matrix to ultimately produce ATP.

Cyto *c* is a soluble protein tethered to the IMM and is responsible for electron shuttling between complex III and complex IV (Acin-Perez et al., 2008). Release of cyto *c* from the mitochondria initiates a cascade of events that are fatal to the cell (Endo et al., 2006; Huttemann et al., 2011). The bulk of cyto *c* is present in the cristae within the mitochondria (Scorrano et al., 2002). Oligomers of OPA1 have been shown to be responsible for maintaining the cristae junction, and disassociation of OPA1 complexes leads to loss of

cristae formation and release of cyto *c* (Yamaguchi et al., 2008; Ramonet et al., 2013). Moreover, the dynamin-like GTPase OPA1 is a central protein of mitochondrial fusion of the IMM (McBride and Soubannier, 2010).

Here we demonstrate the release of cyto *c*, and OPA1 from the mitochondria and the breakdown in OPA1 oligomers following OGD followed by reoxygenation. The release of OPA1 and cyto *c* was concomitant with a dominant fragmented mitochondrial phenotype and ultimately death of neurons. Fragmented or granular mitochondria can result from a breakdown in fusion or an increase in fission. Release of OPA1 from the mitochondria and breakdown in OPA1 oligomers result in unopposed fission, which was visualized as a dominant fragmented phenotype. In fact, Langer's group has shown that common mitochondrial stressors do indeed result in OPA1 processing and mitochondrial fragmentation (Baker et al., 2014). Moreover, OPA1 processing has been shown to be linked to mitochondrial membrane potential (Guillery et al., 2008; Cogliati et al., 2013). Extreme depolarization and hyperpolarization is known to occur during ischemia and reperfusion, respectively. Mitochondria in ischemic vulnerable areas of the brain are susceptible to complete fragmentation (Owens et al., 2015). Furthermore, continuous release of neurotransmitters, a major signaling component of ischemia/reperfusion, induces neuronal death via excitotoxicity. Overexpression of OPA1 restores mitochondrial morphology in NMDA-induced excitoxic cells (Jahani-Asl et al., 2011).

Other proteins known to be involved in mitochondrial dynamics include the fission proteins dynamin related protein 1 (Drp1), mitochondrial fission 1 (Fis1), mitochondrial fission factor (MFF), whereas proteins regarded as responsible for fusion are OPA1, mitofusin 1 and 2 (Mfn1 and Mfn2). Although the physiological environment regulates a balance of mitochondrial fusion and fission, pathological insults typically drive the balance of fusion or fission to either extreme. However, identifying the events that lead to dramatic alterations in mitochondrial phenotype poses a challenge. Interruption of mitochondrial fusion results in a predominantly fission phenotype, and similarly, an increase in the activity of fission proteins would result in the same phenotype. Here we show that there was no change in OPA1 expression, instead there was breakdown in the mitochondrial fusion protein OPA1 and release into the cytosol following OGD with concomitant increase in mitochondrial fragmentation. Similar to our results, Wappler et al. did not measure any alterations in OPA1 expression in whole cell homogenates (Wappler et al., 2013), however they did not investigate OPA1 band pattern alterations in cellular fractions. They go on to report that Drp1 may not be the *major regulator* in the breakdown of the mitochondria, a function they attribute to the mitochondrial fusion protein Mfn1. However, inhibition of the mitochondrial fission protein Drp1 has also been shown to attenuate mitochondrial fission in glutamate stressed HT22 cells and provide neuroprotection in primary neurons exposed to OGD (Grohm et al., 2012). Still, involvement of both Drp1 and OPA1 has been reported to induce the fragmentation of mitochondria in other models of apoptosis (Alaimo et al., 2014). Lack of consensus in these reports in addition to the cell's compensatory mechanisms to experimental alterations in proteins involved in mitochondrial dynamics poses a challenge to researchers in the field. Further investigations will be needed to identify which proteins are

involved in the breakdown of the mitochondria and more importantly, identify potential therapies for the neurodegenerative diseases affected by oxygen deprivation.

CONCLUSION

Our study clearly demonstrates that OPA1 is released from the mitochondria following OGD which is concurrent with fragmented mitochondria. What remains vague is if OPA1 is a transmembrane protein that undergoes proteolytic cleavage or if OPA1 is tethered to the IMM phospholipid cardiolipin that undergoes peroxidation and release OPA1. The mechanism of OPA1 release following ischemia and reperfusion still remains unclear and further studies are needed to elucidate a potential therapeutic target that may attenuate OPA1 and cyto *c* release.

Acknowledgments

Research described in this article was supported by grant NS076715 from the National Institutes of Health (RK, THS).

Abbreviations

BN-PAGE	blue native-polyacrylamide gel electrophoresis
cyto *c*	cytochrome *c*
Drp1	dynamin related protein 1
EDTA	ethylenediaminetetraacetic acid
EGTA	ethylene glycol tetraacetic acid
ETC	electron transport chain
GADPH	glyceraldehyde 3-phosphate dehydrogenase
HEPES	4-(2-hydroxye thyl)-1-piperazineethanesulfonic acid
IMM	inner mitochondrial membrane
LDH	lactate dehydrogenase
Mfn1	mitofusin 1
MIB	mitochondria isolation buffer
mitoGFP	mito green fluorescent protein
OGD	oxygen and glucose deprivation
OPA1	optic atrophy 1
PBS	phosphate-buffered saline
SDS	sodium dodecyl sulfate

REFERENCES

Acin-Perez R, Fernandez-Silva P, Peleato ML, Perez-Martos A, Enriquez JA. Respiratory active mitochondrial supercomplexes. Mol Cell. 2008; 32:529–539. [PubMed: 19026783]

Alaimo A, Gorojod RM, Beauquis J, Munoz MJ, Saravia F, Kotler ML. Deregulation of mitochondria-shaping proteins Opa-1 and Drp-1 in manganese-induced apoptosis. PLoS One. 2014; 9:e91848. [PubMed: 24632637]

Almeida A, Medina JM. Isolation and characterization of tightly coupled mitochondria from neurons and astrocytes in primary culture. Brain Res. 1997; 764:167–172. [PubMed: 9295206]

Almeida A, Medina JM. A rapid method for the isolation of metabolically active mitochondria from rat neurons and astrocytes in primary culture. Brain Res Brain Res Protoc. 1998; 2:209–214. [PubMed: 9507134]

Baker MJ, Lampe PA, Stojanovski D, Korwitz A, Anand R, Tatsuta T, Langer T. Stress-induced OMA1 activation and autocatalytic turnover regulate OPA1-dependent mitochondrial dynamics. EMBO J. 2014; 33:578–593. [PubMed: 24550258]

Bolte S, Cordelieres FP. A guided tour into subcellular colocalization analysis in light microscopy. J Microsc. 2006; 224:213–232. [PubMed: 17210054]

Borutaite V, Jekabsone A, Morkuniene R, Brown GC. Inhibition of mitochondrial permeability transition prevents mitochondrial dysfunction, cytochrome c release and apoptosis induced by heart ischemia. J Mol Cell Cardiol. 2003; 35:357–366. [PubMed: 12689815]

Chan D, Frank S, Rojo M. Mitochondrial dynamics in cell life and death. Cell Death Differ. 2006; 13:680–684. [PubMed: 16410792]

Chen H, Chan DC. Mitochondrial dynamics in mammals. Curr Top Dev Biol. 2004; 59:119–144. [PubMed: 14975249]

Cogliati S, Frezza C, Soriano ME, Varanita T, Quintana-Cabrera R, Corrado M, Cipolat S, Costa V, Casarin A, Gomes LC, Perales-Clemente E, Salviati L, Fernandez-Silva P, Enriquez JA, Scorrano L. Mitochondrial cristae shape determines respiratory chain supercomplexes assembly and respiratory efficiency. Cell. 2013; 155:160–171. [PubMed: 24055366]

Endo H, Kamada H, Nito C, Nishi T, Chan PH. Mitochondrial translocation of p53 mediates release of cytochrome c and hippocampal CA1 neuronal death after transient global cerebral ischemia in rats. J Neurosci. 2006; 26:7974–7983. [PubMed: 16870742]

Grohm J, Kim SW, Mamrak U, Tobaben S, Cassidy-Stone A, Nunnari J, Plesnila N, Culmsee C. Inhibition of Drp1 provides neuroprotection in vitro and in vivo. Cell Death Differ. 2012; 19:1446–1458. [PubMed: 22388349]

Guillery O, Malka F, Landes T, Guillou E, Blackstone C, Lombes A, Belenguer P, Arnoult D, Rojo M. Metalloproteinase-mediated OPA1 processing is modulated by the mitochondrial membrane potential. Biol Cell. 2008; 100:315–325. [PubMed: 18076378]

Hilgenberg LG, Smith MA. Preparation of dissociated mouse cortical neuron cultures. J Vis Exper. 2007:562. [PubMed: 18989405]

Hirakawa A, Takeyama N, Nakatani T, Tanaka T. Mitochondrial permeability transition and cytochrome c release in ischemia-reperfusion injury of the rat liver. J Surg Res. 2003; 111:240–247. [PubMed: 12850469]

Hornig-Do HT, Gunther G, Bust M, Lehnartz P, Bosio A, Wiesner RJ. Isolation of functional pure mitochondria by superparamagnetic microbeads. Anal Biochem. 2009; 389:1–5. [PubMed: 19285029]

Huttemann M, Pecina P, Rainbolt M, Sanderson TH, Kagan VE, Samavati L, Doan JW, Lee I. The multiple functions of cytochrome c and their regulation in life and death decisions of the mammalian cell: from respiration to apoptosis. Mitochondrion. 2011; 11:369–381. [PubMed: 21296189]

Jahani-Asl A, Pilon-Larose K, Xu W, MacLaurin JG, Park DS, McBride HM, Slack RS. The mitochondrial inner membrane GTPase, optic atrophy 1 (Opa1), restores mitochondrial morphology and promotes neuronal survival following excitotoxicity. J Biol Chem. 2011; 286:4772–4782. [PubMed: 21041314]

Kristian T, Hopkins IB, McKenna MC, Fiskum G. Isolation of mitochondria with high respiratory control from primary cultures of neurons and astrocytes using nitrogen cavitation. J Neurosci Methods. 2006; 152:136–143. [PubMed: 16253339]

McBride H, Soubannier V. Mitochondrial function: OMA1 and OPA1, the grandmasters of mitochondrial health. Curr Biol. 2010; 20:R274–276. [PubMed: 20334834]

Namura S, Nagata I, Takami S, Masayasu H, Kikuchi H. Ebselen reduces cytochrome c release from mitochondria and subsequent DNA fragmentation after transient focal cerebral ischemia in mice. Stroke. 2001; 32:1906–1911. [PubMed: 11486124]

Nguyen D, Alavi MV, Kim KY, Kang T, Scott RT, Noh YH, Lindsey JD, Wissinger B, Ellisman MH, Weinreb RN, Perkins GA, Ju WK. A new vicious cycle involving glutamate excitotoxicity, oxidative stress and mitochondrial dynamics. Cell Death Dis. 2011; 2:e240. [PubMed: 22158479]

Owens K, Park JH, Gourley S, Jones H, Kristian T. Mitochondrial dynamics: cell-type and hippocampal region specific changes following global cerebral ischemia. J Bioenerg Biomembr. 2015; 47:13–31. [PubMed: 25248415]

Perez-Pinzon MA, Xu GP, Born J, Lorenzo J, Busto R, Rosenthal M, Sick TJ. Cytochrome c is released from mitochondria into the cytosol after cerebral anoxia or ischemia. J Cereb Blood Flow Metab. 1999; 19:39–43. [PubMed: 9886353]

Perkins G, Renken C, Martone ME, Young SJ, Ellisman M, Frey T. Electron tomography of neuronal mitochondria: three-dimensional structure and organization of cristae and membrane contacts. J Struct Biol. 1997; 119:260–272. [PubMed: 9245766]

Prakasa Babu P, Yoshida Y, Su M, Segura M, Kawamura S, Yasui N. Immunohistochemical expression of Bcl-2, Bax and cytochrome c following focal cerebral ischemia and effect of hypothermia in rat. Neurosci Lett. 2000; 291:196–200. [PubMed: 10984640]

Ramonet D, Perier C, Recasens A, Dehay B, Bove J, Costa V, Scorrano L, Vila M. Optic atrophy 1 mediates mitochondria remodeling and dopaminergic neurodegeneration linked to complex I deficiency. Cell Death Differ. 2013; 20:77–85. [PubMed: 22858546]

Sanderson TH, Kumar R, Sullivan JM, Krause GS. Insulin blocks cytochrome c release in the reperfused brain through PI3-K signaling and by promoting Bax/Bcl-XL binding. J Neurochem. 2008; 106:1248–1258. [PubMed: 18518905]

Sanderson TH, Mahapatra G, Pecina P, Ji Q, Yu K, Sinkler C, Varughese A, Kumar R, Bukowski MJ, Tousignant RN, Salomon AR, Lee I, Huttemann M. Cytochrome c is tyrosine 97 phosphorylated by neuroprotective insulin treatment. PLoS One. 2013; 8:e78627. [PubMed: 24223835]

Sanderson TH, Raghunayakula S, Kumar R. Release of mitochondrial Opa1 following oxidative stress in HT22 cells. Mol Cell Neurosci. 2015; 64:116–122. [PubMed: 25579226]

Scorrano L, Ashiya M, Buttle K, Weiler S, Oakes SA, Mannella CA, Korsmeyer SJ. A distinct pathway remodels mitochondrial cristae and mobilizes cytochrome c during apoptosis. Dev Cell. 2002; 2:55–67. [PubMed: 11782314]

Scorziello A, Pellegrini C, Forte L, Tortiglione A, Gioielli A, Iossa S, Amoroso S, Tufano R, Di Renzo G, Annunziato L. Differential vulnerability of cortical and cerebellar neurons in primary culture to oxygen glucose deprivation followed by reoxygenation. J Neurosci Res. 2001; 63:20–26. [PubMed: 11169610]

Sugawara T, Fujimura M, Morita-Fujimura Y, Kawase M, Chan PH. Mitochondrial release of cytochrome c corresponds to the selective vulnerability of hippocampal CA1 neurons in rats after transient global cerebral ischemia. J Neurosci. 1999; 9:RC39. [PubMed: 10559429]

Wappler EA, Institoris A, Dutta S, Katakam PV, Busija DW. Mitochondrial dynamics associated with oxygen–glucose deprivation in rat primary neuronal cultures. PLoS One. 2013; 8:e63206. [PubMed: 23658809]

Yamaguchi R, Lartigue L, Perkins G, Scott RT, Dixit A, Kushnareva Y, Kuwana T, Ellisman MH, Newmeyer DD. Opa1-mediated cristae opening is Bax/Bak and BH3 dependent, required for apoptosis, and independent of Bak oligomerization. Mol Cell. 2008; 31:557–569. [PubMed: 18691924]

Zhao H, Yenari MA, Cheng D, Sapolsky RM, Steinberg GK. Biphasic cytochrome c release after transient global ischemia and its inhibition by hypothermia. J Cereb Blood Flow Metab. 2005; 25:1119–1129. [PubMed: 15789032]

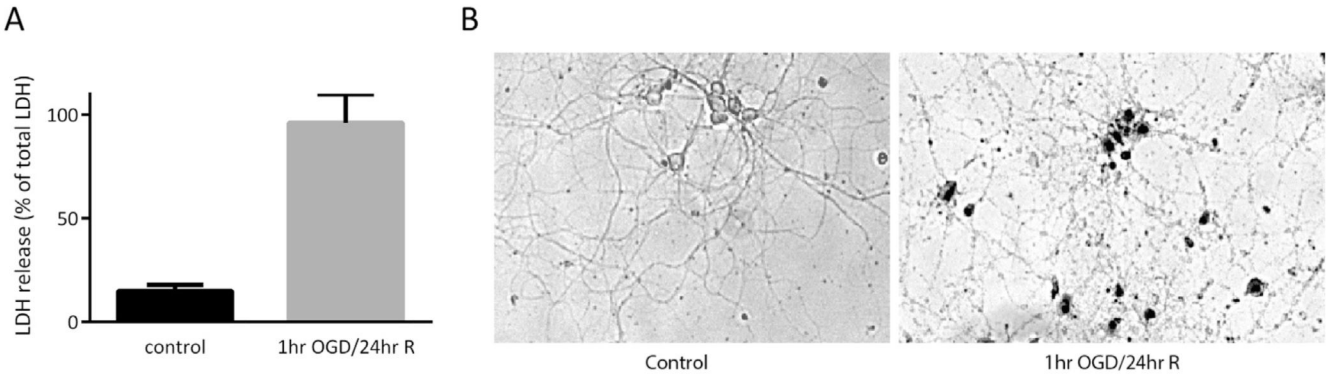

Fig. 1.

Oxygen glucose deprivation induces cell death. Primary neurons were subjected to one hour of oxygen glucose deprivation followed by 24 h of reoxygenation in glucose rich media. LDH release was measured in the media of control and experimental groups and normalized to total LDH release. This insult produces a significant increase in cell death compared to control as measured by LDH release assay (A, $p < 0.05$). Trypan blue was utilized to validate neuronal death and examine the overall morphological alteration to neurons (B).

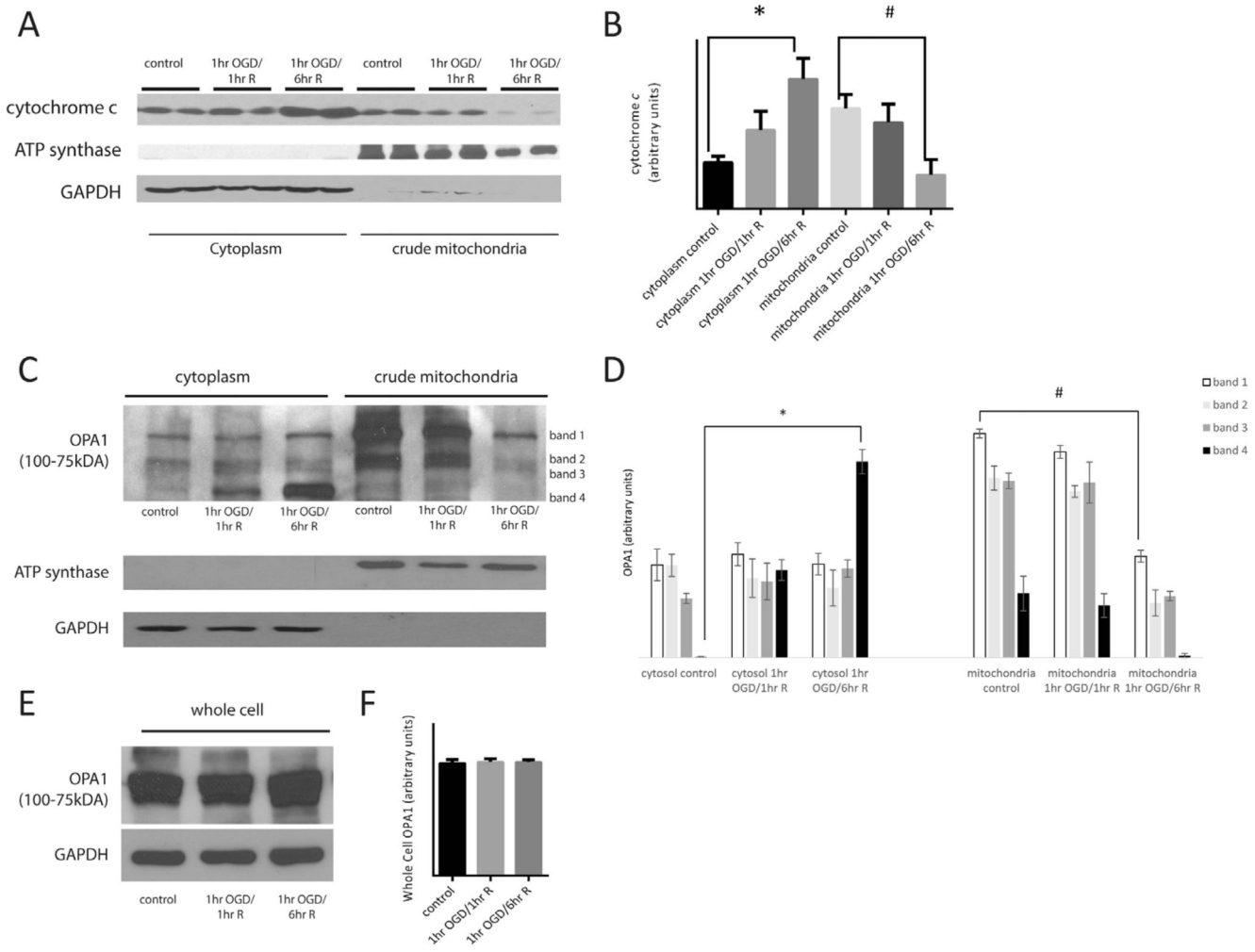

Fig. 2.

Oxygen glucose deprivation triggers cytochrome *c* and OPA1 release. Primary neurons were subjected to 1 h of OGD followed by 1 or 6 h of reoxygenation in glucose rich media. Cells were separated into a cytoplasm and crude mitochondrial fractions. Proteins were resolved using SDS-PAGE followed by Western blot analysis probing for cyto *c* (A) and OPA1 (C, E). In control cells, cyto *c* is present in the crude mitochondria fraction, however following 6-h reoxygenation, cyto *c* has largely shifted to the cytoplasmic fraction (A, B; $p < 0.05$). OPA1 exists in several long and short isoforms between 75 and 100 kDa. In control cells, higher molecular weight OPA1 isoforms are predominantly in the mitochondria (C; bands 1-3). Following 1-h OGD and 6-h reoxygenation, there is loss of OPA1 from the mitochondria with a significant increase in the lower molecular weight isoform (band 4) in the cytoplasm (C, D; $p < 0.05$). OPA1 protein expression was measured in whole cell homogenates in control and experimental groups and there was no significant change in OPA1 (E, F; $p < 0.05$).

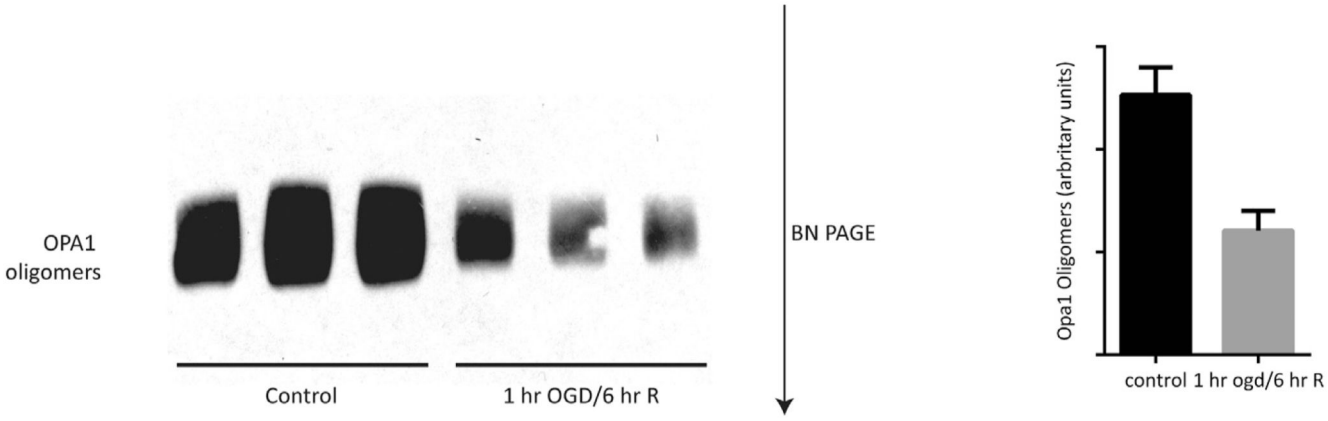

Fig. 3.

Oxygen glucose deprivation results in breakdown of OPA1 oligomers. Primary neurons were subjected to 1 h of OGD followed by 6 h of reoxygenation in glucose rich media. The molecular mass and oligomeric state of OPA1 membrane protein complexes were analyzed using BN-PAGE. Following OGD and reoxygenation, there is significant reduction of OPA1 oligomers compared to control samples ($p < 0.05$).

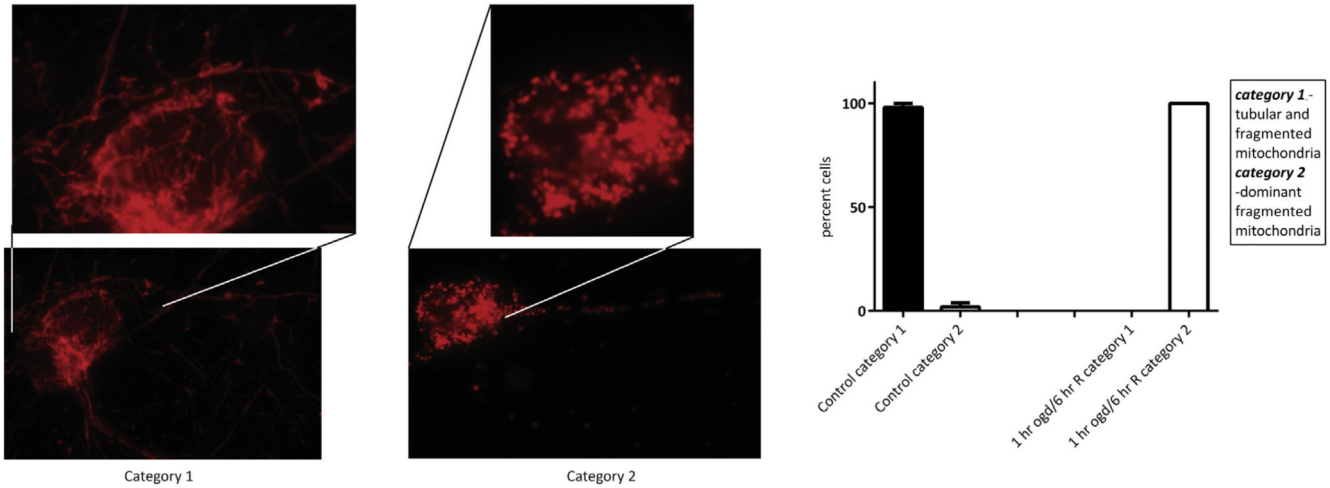

Fig. 4.

Oxygen glucose deprivation results in fragmented mitochondria. Mitochondrial morphology was visualized using Mitotracker Red. In control cells, mitochondria appear interconnected, thread-like and are present throughout the soma and the processes. However, following OGD and reoxygenation, mitochondrial morphology is dramatically altered to a small granular phenotype (fragmentation) that is localized to the soma. Neurons were characterized according to mitochondrial morphology. Following 1-h OGD and 6-h of reoxygenation, there was a significant increase in cells displaying fragmented mitochondria ($p < 0.05$) and an analogous decrease in the number of cells displaying interconnected, thread-like mitochondria. (For interpretation of the references to colour in this figure legend, the reader is referred to the web version of this article.)

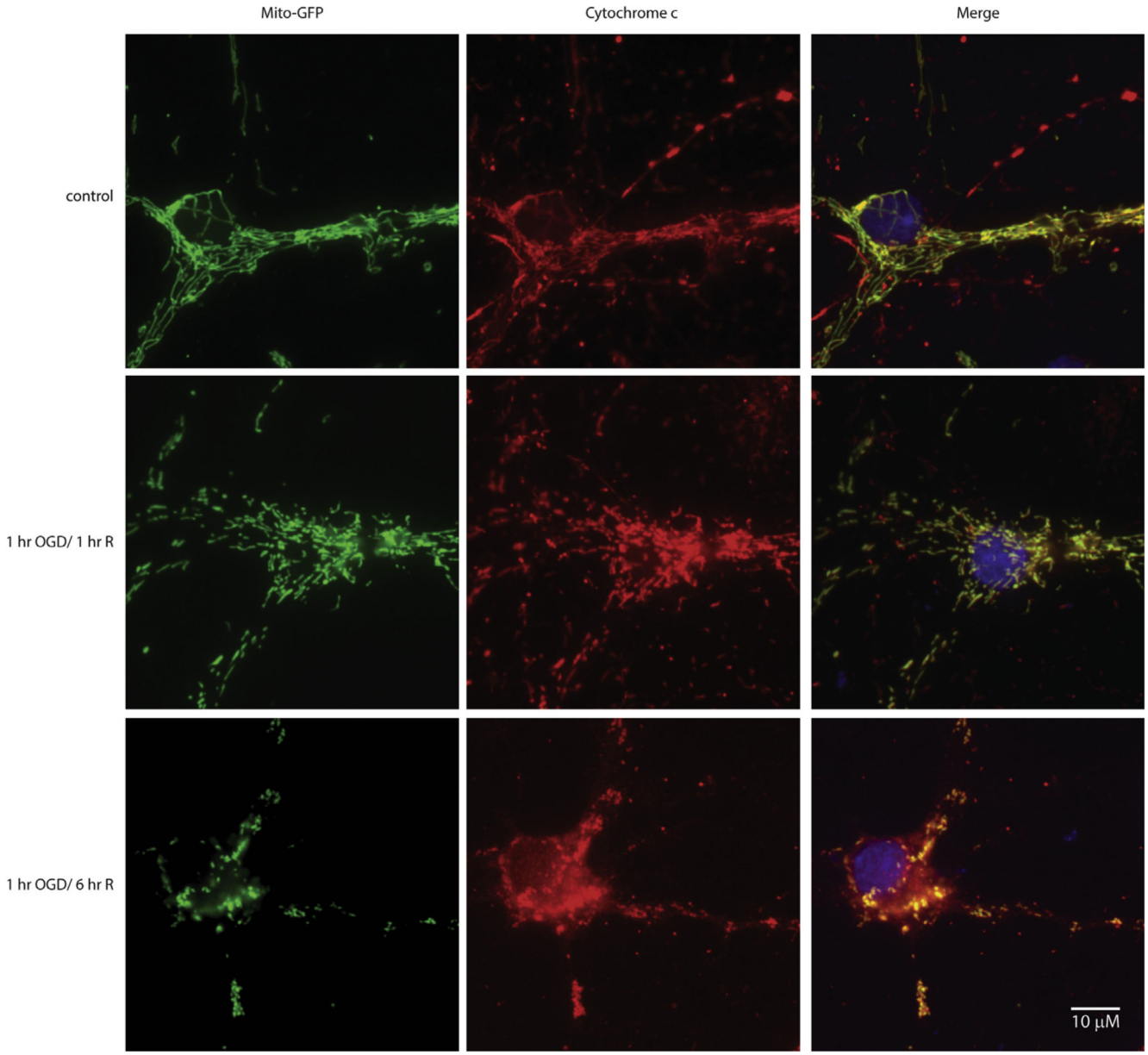

Fig. 5.

Oxygen glucose deprivation results release of cytochrome *c* from the mitochondria. Mitochondrial targeted GFP transfected primary neurons (column 1) were subjected to 1 h of OGD followed by 1 or 6 h of reoxygenation in glucose rich media. Following fixation, an antibody directed against cytochrome *c* (red; column 2) was used to identify localization. The yellow signal in the merged overlay indicates co-localization (column 3). In control cells (row 1), cytochrome *c* immunofluorescence had absolute overlay with mitochondrial GFP signal as seen in the merged column. Following 1-h OGD and 1-h reoxygenation in glucose rich media (row 2), mitochondrial morphology differed from the controls, however, cytochrome *c* signal co-localized with mitochondria. However, 1-h OGD followed by 6-h reoxygenation (row 3) resulted in widespread cytochrome *c* signal in the cytoplasm, with

fragmented mitochondria. (For interpretation of the references to colour in this figure legend, the reader is referred to the web version of this article.)